Transport to the plasma membrane is regulated differently early and late in the cell cycle in *Saccharomyces cerevisiae*

Bettina Zanolari[1,*], Uli Rockenbauch[1,*], Mark Trautwein[1], Lorena Clay[2], Yves Barral[2] and Anne Spang[1,‡]

[1]Biozentrum, University Basel, CH-4056 Basel, Switzerland
[2]ETH Zürich Hönggerberg, CH-8049 Zürich, Switzerland

*These authors contributed equally to this work
‡Author for correspondence (anne.spang@unibas.ch)

Accepted 13 November 2010
Journal of Cell Science 124, 1055-1066

doi:10.1242/jcs.072371

Summary

Traffic from the *trans*-Golgi network to the plasma membrane is thought to occur through at least two different independent pathways. The chitin synthase Chs3p requires the exomer complex and Arf1p to reach the bud neck of yeast cells in a cell-cycle-dependent manner, whereas the hexose transporter Hxt2p localizes over the entire plasma membrane independently of the exomer complex. Here, we conducted a visual screen for communalities and differences between the exomer-dependent and exomer-independent transport to the plasma membrane in *Saccharomyces cerevisiae*. We found that most of the components that are required for the fusion of transport vesicles with the plasma membrane, are involved in localization of both Chs3p and Hxt2p. However, the lethal giant larva homologue Sro7p is required primarily for the targeting of Chs3p, and not Hxt2p or other cargoes such as Itr1p, Cwp2p and Pma1p. Interestingly, this transport defect was more pronounced in large-budded cells just before cytokinesis than in small-budded cells. In addition, we found that the yeast Rab11 homologue Ypt31p determines the residence time of Chs3p in the bud neck of small-budded, but not large-budded, cells. We propose that transport to and from the bud neck is regulated differently in small- and large-budded cells, and differs early and late in the cell cycle.

Key words: Small GTPases, Intracellular traffic, Cell cycle, Yeast, Exocytosis, Endocytosis

Introduction

Various transport pathways operate to localize cargo to the plasma membrane. At least two different transport pathways have been identified in yeast by the buoyant density of the transport carriers and the cargo they contain (Gurunathan et al., 2002; Harsay and Bretscher, 1995; Harsay and Schekman, 2002). The high-density fraction transports exoglucanase and invertase, whereas the low-density pool brings the plasma membrane ATPase Pma1p, the glucose transporter Hxt2p, Fus1p and the chitin synthase III Chs3p, and probably a large variety of other cargo to the plasma membrane (Bagnat and Simons, 2002; Barfield et al., 2009; Harsay and Schekman, 2002; Kruckeberg et al., 1999). The lighter pool of transport containers can probably be further split into subclasses. Chs3p and Fus1p have distinct transport requirements from Pma1p or Hxt2p, because they need the action of the exomer complex for exit from the *trans*-Golgi network (TGN) (Sanchatjate and Schekman, 2006; Trautwein et al., 2006; Wang et al., 2006). The exomer complex consists of the peripheral Golgi protein Chs5p and the ChAP proteins (Wang et al., 2006). The ChAPs are four homologous proteins that can interact with both the small GTPase Arf1p and Chs5p (Trautwein et al., 2006). They form complexes of varying stoichiometries and might act as receptors for cargoes to be transported by the exomer-dependent pathway (Sanchatjate and Schekman, 2006; Trautwein et al., 2006). Whether exomer is a sorting complex at the TGN, similarly to the ESCRTIII complex at the endosome (Saksena et al., 2009) or a novel coat, remains to be established. The exomer complex fulfils two of the hallmarks of a vesicle coat because it interacts directly with both a small GTPase of the Arf/Sar family and cargo proteins (Trautwein et al., 2006). However, unlike the COPI and COPII coats (Matsuoka et al., 1998; Spang et al., 1998), the exomer complex, with Arf1p, fails to change the membrane curvature of liposomes or to bud off vesicles (Wang et al., 2006).

Chs3p displays an interesting localization pattern as it changes over the cell-cycle. Early in the cell-cycle in G1 and S phase, Chs3p is located at the incipient bud site and at the bud neck of small-budded cells. In G2, when the bud is medium sized, Chs3p is present in internal structures referred to as chitosomes (Chuang and Schekman, 1996; Ziman et al., 1996), which are endosomes. In mitosis, when also the actin cytoskeleton re-polarizes from the bud tip to the bud neck, Chs3p is exported to the bud neck again. By contrast, the fusion of secretory transport vesicles is thought to occur at the incipient bud site and then in G1 and S phase of the cell cycle, at the bud tip. During G2, vesicles fuse all over the bud surface and subsequently, during cytokinesis, relocalization of the vesicle fusion site to the bud neck occurs. This raises the question whether fusion of Chs3p-containing transport vesicles is governed by the same regulatory factors as that of general transport vesicles. It is assumed that the exocyst is required for fusion of transport vesicles with the plasma membrane because mutants in the exocyst component *SEC6* accumulate vesicles (TerBush et al., 1996), some of which contain Chs3p (Valdivia et al., 2002). However, no detailed analysis is available.

Here, we investigate how the transport of Chs3p to the bud neck region of the plasma membrane is controlled in *Saccharomyces cerevisiae*. We show that delivery of Chs3p to the bud neck region

continues, even when the vesicle fusion machinery is only apparent in the bud tip. To gain a better understanding of the regulation of Chs3p localization at the plasma membrane, we performed a visual screen comparing the transport of Chs3p and Hxt2p to the plasma membrane using fluorescently labeled variants. We found that the general fusion machinery at the plasma membrane is essential for the efficient delivery of both cargoes to the plasma membrane, independent of whether the cargo is localized to the bud neck region or the entire plasma membrane. However, some transport mutants affected the localization of Chs3p and Hxt2p, and other exomer-independent cargo differentially. Moreover, we found that the residence time of Chs3p at the bud neck is determined in different ways in small- and large-budded cells. Our data therefore indicate that general transport factors can selectively influence the temporal and spatial localization of different cargoes.

Results

Transport dynamics of Chs3p and the exocyst complex over the yeast cell cycle

To gain further insight into the temporal and spatial aspects of Chs3p transport, we observed localization of Chs3p–GFP over the cell cycle. As reported previously (Valdivia et al., 2002), Chs3p–GFP is present in the bud-neck in small-budded cells immediately after bud emergence (G1–S phase), it disappears from the bud neck in medium-budded cells (G2 phase), to reappear only in the bud neck of large-budded cells (M-phase), where it persists until the end of cytokinesis (Fig. 1A). Transport vesicles generally fuse at the bud tip of small-budded cells, all over the bud surface in medium-sized cells and then vesicle fusion is restricted to the bud neck region at cytokinesis. The site of vesicle fusion is marked by the presence of the exocyst complex, which serves as tethering complex for vesicles with the plasma membrane (Guo et al., 1999). We used Sec8p, a member of the exocyst complex (TerBush and Novick, 1995), fused to GFP to visualize the localization of the exocyst complex over the cell cycle (Fig. 1A). Sec8p–GFP was functional because a chromosomal fusion to the essential *SEC8* was generated at the endogenous locus, and the resulting strain grew indistinguishably from an untagged control. Interestingly, Chs3p–GFP remained restricted to the bud neck when the fusion machinery was localized to the bud tip. This observation could be explained by two different possibilities. First, Chs3p–GFP transport is restricted to the short time-window of initiation of bud emergence. Second, Chs3p–GFP transport to the bud neck persists after bud emergence. In the latter case, Chs3p could be delivered either directly to the bud neck or to the bud tip and then a 'diffusion-and-trapping' mechanism would anchor Chs3p at the bud neck. To determine whether Chs3p could be delivered to the bud neck after the initial bud growth had been initiated, we performed a FRAP analysis. We bleached the Chs3p–GFP signal in small-budded cells and determined the reappearance of the Chs3p–GFP signal in the bud neck 10 minutes after the initial bleaching (Fig. 1B). In 80% (n=16) of the small-budded cells, we observed reappearance of the Chs3p signal in the bud neck after photobleaching, indicating that Chs3p pools at the plasma membrane can be replenished after initiation of the budding process.

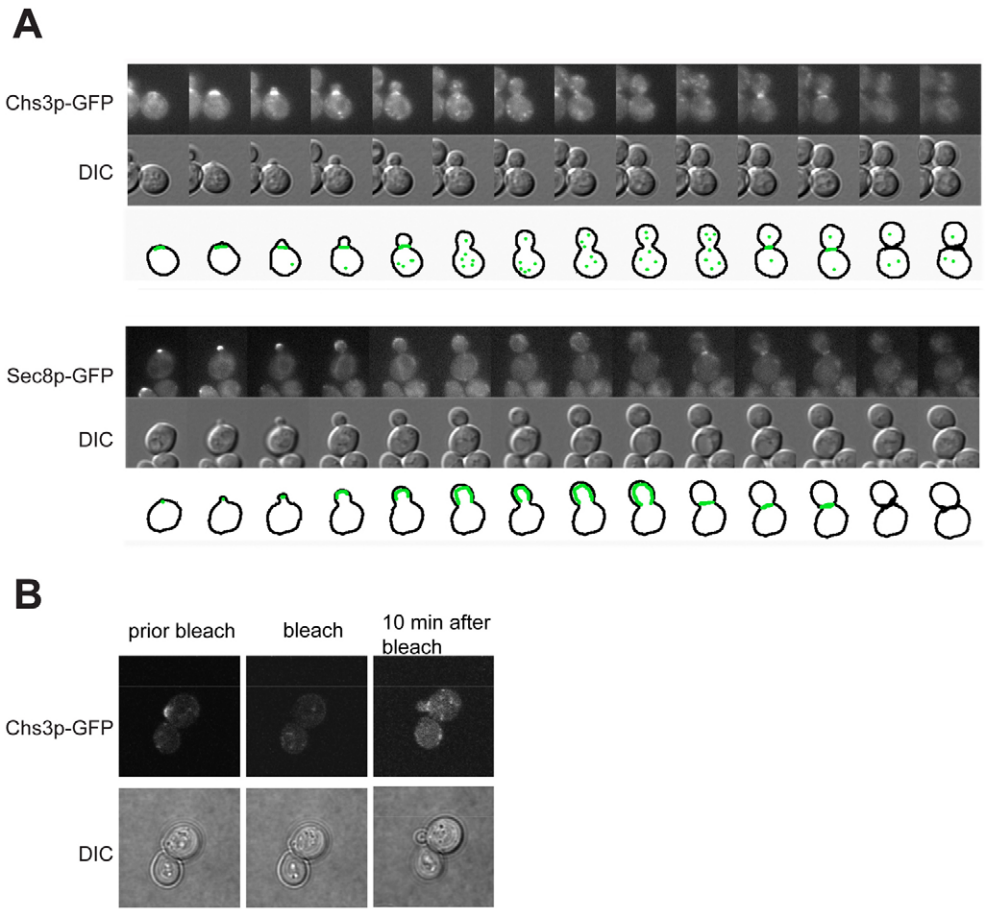

Fig. 1. Cell-cycle-dependent transport of Chs3p–GFP. (**A**) Time-lapse images of wild-type yeast cells bearing either Chs3p–GFP or Sec8p–GFP. The images in the DIC and GFP channels were acquired every 10 minutes. The schematic drawings underneath the time-lapse images illustrate the localization of the GFP-tagged proteins. (**B**) Chs3p–GFP reaches the bud neck even after bud emergence in small-budded cells. Cells expressing Chs3p–GFP, which had just initiated bud formation were used for FRAP experiments. A *Z*-stack was acquired before and 10 minutes after bleaching the incipient bud site. For the analysis, cells were taken into account in which the bud grew during the 10 minute period after the bleaching. Representative single plane images are shown.

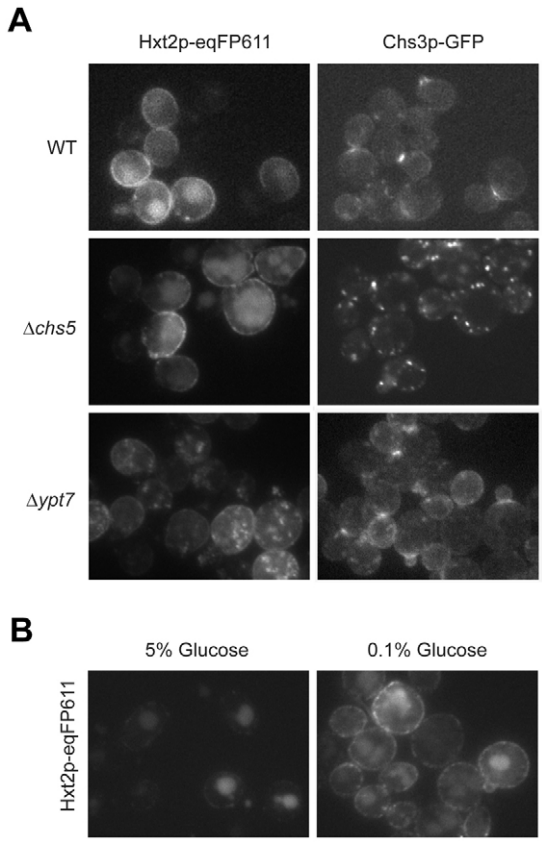

Fig. 2. Trafficking of Hxt2p–eqFP611 and Chs3p–GFP. (**A**) Hxt2p–eqFP611 and Chs3p–GFP have different requirements for plasma membrane localization. Chs3p–GFP and Hxt2p–eqFP611 were expressed from their endogenous loci in different strains. Chs3p–GFP was specifically retained in *Δchs5* cells, whereas prominent mislocalization of Hxt2p–eqFP611 was observed in *Δypt7* cells. (**B**) Hxt2p–eqFP611 is exported to the plasma membrane upon shift from high-glucose to low-glucose medium. Cells were grown to log phase in medium containing 5% glucose at 30°C, harvested and resuspended in medium with 0.1% glucose and incubated again. The images were acquired 1.5 hours after downshift.

Chs3p and Hxt2p travel independently to the plasma membrane

To gain a better understanding of the plasma membrane localization of Chs3p, we used a strain in which Chs3p was appended with 2×GFP and the plasma-membrane-localized hexose transporter Hxt2p with the red fluorescent protein eqFP611 (Wiedenmann et al., 2002) (Fig. 2A). We decided to use Hxt2p because it can be used for steady state as well as pulse–chase analysis (Kruckeberg et al., 1999). In medium containing high levels of glucose (5%) Hxt2p did not localize to the plasma membrane, but was instead routed to the vacuole (Fig. 2B). Upon shift to low-glucose medium (0.1% glucose), Hxt2p was transported to the plasma membrane. Therefore, Hxt2p provides a suitable cargo model for steady state and pulse analysis. Hxt2p localization is independent of exomer because in a *Δchs5* mutant, in which Chs3p–GFP is retained in the Golgi, Hxt2p–eqFP611 still reached the plasma membrane under normal and low-glucose conditions (Fig. 2A, Table 1 and data not shown). Conversely, in a *Δypt7* strain, in which Chs3p–GFP traffic is only mildly affected, Hxt2p–eqFP611 staining at the plasma membrane was clearly reduced, and the protein was instead enriched in the vacuole (which is fragmented in the absence of Ypt7p) (Fig. 2A). The mislocalization of Hxt2p in *Δypt7* was specific and no significant changes in plasma membrane localization were observed for the plasma membrane ATPase Pma1p, the GPI-anchored cell-wall protein Cwp2p or the inositol transporter Itr1p (supplementary material Fig. S1) (Table 1). By contrast, as expected, the vacuolar carboxypeptidase Y (CPY) showed abnormal localization in *Δypt7* cells (supplementary material Fig. S1) (Table 1). These data demonstrate, that Chs3p and Hxt2p have different requirements to ensure their proper delivery to the plasma membrane.

The exocyst is required for localization of Chs3p–GFP to the bud neck

First, we wanted to investigate whether both Hxt2p transport and Chs3p traffic requires the same exocyst tethering complex. All exocyst components are essential and therefore deletions are not available. The use of temperature-sensitive strains for the investigation of Chs3p traffic is limited because Chs3p is involved in acute heat-shock response (Fig. 3A) (Valdivia and Schekman, 2003). Upon shift of wild-type cells to 37°C, Chs3p was rapidly endocytosed and appeared at the plasma membrane in a delocalized manner. After 2.5 hours at 37°C, cells had adapted to the new environment and Chs3p relocated to the bud neck. Therefore, upon shift of temperature-sensitive mutant cells to the restrictive temperature (37°C), we would only be able to observe the effect of mutants on heat-shock-induced trafficking of Chs3p, and not its normal delivery to the bud neck. However, some temperature-sensitive mutants show an effect at the permissive temperature (23°C). Thus, we determined the localization of Chs3p–GFP and Hxt2p–eqFP611 in exocyst mutants at 23°C. Whereas *sec6-4* cells showed wild-type localization of both markers, Chs3p–GFP was at least partially delocalized over the plasma membrane in *sec3-2* cells. Under these conditions, Hxt2p–eqFP611 was still properly localized (Fig. 3A) (Table 1). To corroborate the transport defect, we screened more temperature-sensitive transport mutants for a transport defect at the permissive (23°C) or semi-permissive temperature (30°C) using Pma1p–GFP, Itr1p–GFP and GFP–Cwp2p as markers. While *sec5-24* showed no transport defect at the indicated temperatures, *sec10-2* showed aberrant localizations of the markers at 30°C and *exo84-117* at 23°C (Fig. 3B) (Table 1). As expected, localization of Chs3p–GFP at the bud neck was impaired under the same conditions in which the other markers had failed to localize properly (Fig. 3B,C) (Table 1). More importantly, *sec5-24* cells failed to correctly localize Chs3p–GFP to the bud neck at 30°C, indicating that Chs3p localization is strongly dependent on a functional exocyst complex. Moreover, the data suggest, that Chs3p trafficking might be more sensitive to non-functional exocyst than other cargo transported to the bud tip.

Another way to test for exocyst requirement in Chs3p transport is to selectively downregulate one of its components. To this end, we constructed a strain in which *SEC6* is under *GAL1* promoter control and Chs3p is tagged with GFP, and performed a *GAL1* shut-off experiment. Growth of this strain in glucose represses the *GAL1* promoter and leads to a depletion of Sec6p. After 13 hours of growth in glucose-containing medium, when about 70% of the cells were still alive (data not shown), Chs3p–GFP was found in a diffuse pattern in the cells, indicating that Chs3p was trapped in vesicles that failed to fuse with the plasma membrane (Fig. 3D). This result is consistent with the absence of exocyst function and hence the accumulation of vesicles in the cell. This accumulation

Table 1. Summary of localization phenotypes in various mutants

Genotype	Function	Correct localization					
		Chs3p	Hxt2p	Cwp2	Pma1p	Itr1p	CPY
WT		++	++	++	++	++	++
Δchs5	Chs3p trafficking to bud neck	– –	++	++	++	++	++
Δypt6	Intra Golgi trafficking	+	+	ND	ND	ND	ND
Δypt7	LE>Lysosome	+	–	++	++	++	–
Δypt10	Endosomal transport	+	++	ND	ND	ND	ND
Δypt11	Organelle inheritance	+	++	ND	ND	ND	ND
Δypt51	EE>LE, TGN>LE	++	+	ND	ND	ND	ND
Δypt51/Δypt52/Δypt53	EE>LE, TGN>LE	– –	–	–	–	–	+
Δmsb3	GAP of Sec4p	++	++	ND	ND	ND	ND
Δmsb4	GAP of Sec4p	+	++	ND	ND	ND	ND
Δmsb3/Δmsb4	GAP of Sec4p	– –	– –	ND	ND	ND	ND
Δsro7	Regulation of exocytosis	–	++	+	++	–[a] ++[b]	++
Δsro77	Regulation of exocytosis	+	++	++	++	++	++
Δsro7/Δsro77	Regulation of exocytosis	– –	– –	–	–	+	+
Δbni4	Anchoring of Chs3p at bud neck	–	ND	ND	ND	ND	ND
Δchs4	Activation of Chs3p at bud neck	–	ND	ND	ND	ND	ND
Δbni4/Δchs4	Function of Chs3p at bud neck	– –	ND	ND	ND	ND	ND
Δypt31	TGN>PM	–	++	+	++	+	++
Δypt32	TGN>PM	+	++	++	++	++	++
Δsur2	Sphingolipid synthesis	++	++	ND	ND	ND	ND
Δelo3	Sphingolipid synthesis	+	+	ND	ND	ND	ND
Δypt31/ypt32A141D[c]	TGN>PM	++	+	ND	++	+	ND
Δypt31/ypt32A141D[d]	TGN>PM	– –	–	–	–	+	ND
sec6-4[c]	Exocyst	++	++	ND	ND	ND	ND
sec3-2[c]	Exocyst	+	++	ND	ND	ND	ND
sec5-24[d]	Exocyst	–	ND	+	+	+	ND
sec10-2[c]	Exocyst	–	ND	+	++	+	ND
sec10-2[d]	Exocyst	– –	ND	– –	–	– –	ND
exo-84-117[c]	Exocyst	–	ND	–	+	+	ND
exo-84-117[d]	Exocyst	– –	ND	– –	–	–	ND
sec4-8[c]	Golgi>PM	–	++	ND	ND	ND	ND
sec2-41[c]	GEF for Sec4p	–	++	ND	ND	ND	ND
ypt1-3[c]	ER>Golgi	++	++	ND	ND	ND	ND

++, Localization indistinguishable from wild type; + slight changes in localization or mislocalization in ≤10% of cells; –, obvious changes in localization or mislocalization in a large number of cells; – –, strong mislocalization defect in almost all (or all) cells. [a]Early chase times; [b]late chase times and steady state; [c]temperature-sensitive mutants, tested at 23°C; [d]temperature-sensitive mutants, tested at 30°C (semi-permissive temperature).

of vesicles has been demonstrated in vitro by gradient fractionation of a *sec6-4* strain after shift for 1 hour to the non-permissive temperature (Valdivia et al., 2002). Chs3p–GFP co-migrated with the plasma membrane marker Pma1p in the vesicle fraction upon depletion of Sec6p by incubating a strain containing *SEC6* under the control of the *GAL1* promoter in medium containing glucose (Fig. 4). In a wild-type strain, this peak was not observed because no transport vesicles accumulate. Moreover, growing the cells in galactose, which keeps the promoter active did not interfere with plasma membrane transport (Fig. 4).

To extend our finding on the exocyst requirement for localization of Chs3p at the bud neck, we used mutant exocyst-associated proteins. The lethal giant larva homologue Sro7p and its close homologue Sro77p appear to bridge the interaction between the t-SNARE in the plasma membrane, Sec9p and the exocyst. Deletions of *SRO7* and *SRO77* are viable, and the growth of the double deletion is strongly impaired. In a *Δsro7* strain, Chs3p–GFP was enriched in internal structures, whereas Hxt2p–eqFP611 was properly localized (Fig. 5A, Table 1). This phenotype seemed to be more pronounced in large-budded than in small-budded cells (Fig. 5B). The effect on transport of Chs3p–GFP in *Δsro7* cells was specific, because Hxt2p–eqFP611 was also exported to the plasma membrane after shift from high-glucose to low-glucose medium (Fig. 5C). In the double deletion *Δsro7 Δsro77*, both markers were aberrantly localized under normal growth conditions, which is consistent with the notion that Sro7p and Sro77p have overlapping functions. Interestingly, under the high-to-low glucose regime, Hxt2p–eqFP611 was efficiently exported to the plasma membrane even in a *Δsro7 Δsro77* strain (Fig. 5C), indicating that under these conditions Hxt2p was routed into a Sro7/Sro77p-independent pathway. This prompted us to test another cargo, Itr1p, whose transport to the plasma membrane is dependent on inositol availability. Little Itr1p–GFP is found at the plasma membrane when cells are grown in rich medium. However, growth in minimal medium causes the inositol transporter to be efficiently expressed at the plasma membrane (Miyashita et al., 2003) (Fig. 5D). At steady state conditions, the localization of Itr1p was not compromised by the loss of either *SRO7* or *SRO77* (Fig. 5E), yet in *Δsro7 Δsro77* cells Itr1p–GFP was partially mislocalized, to a much lower extent than that observed for Hxt2p–eqFP611 (Table 1). By contrast, when we shifted *Δsro7* cells from rich medium to minimal medium and determined Itr1p–GFP localization after 20 minutes, Itr1p did not efficiently reach the plasma membrane in 10–20% of the cells (Fig. 5F). Interestingly, 1.5 hours after the shift, this partial mislocalization defect was rescued, indicating that vesicle fusion with the plasma membrane is slowed down in *Δsro7* cells, but is not detectable for cargo that is continuously present in large amounts at the plasma membrane, or which is cycling very slowly. Most important, however, is the observation that while mislocalized Itr1p–GFP appeared as a haze mostly distributed over the entire cell irrespective of the cell cycle stage, Chs3p–GFP was

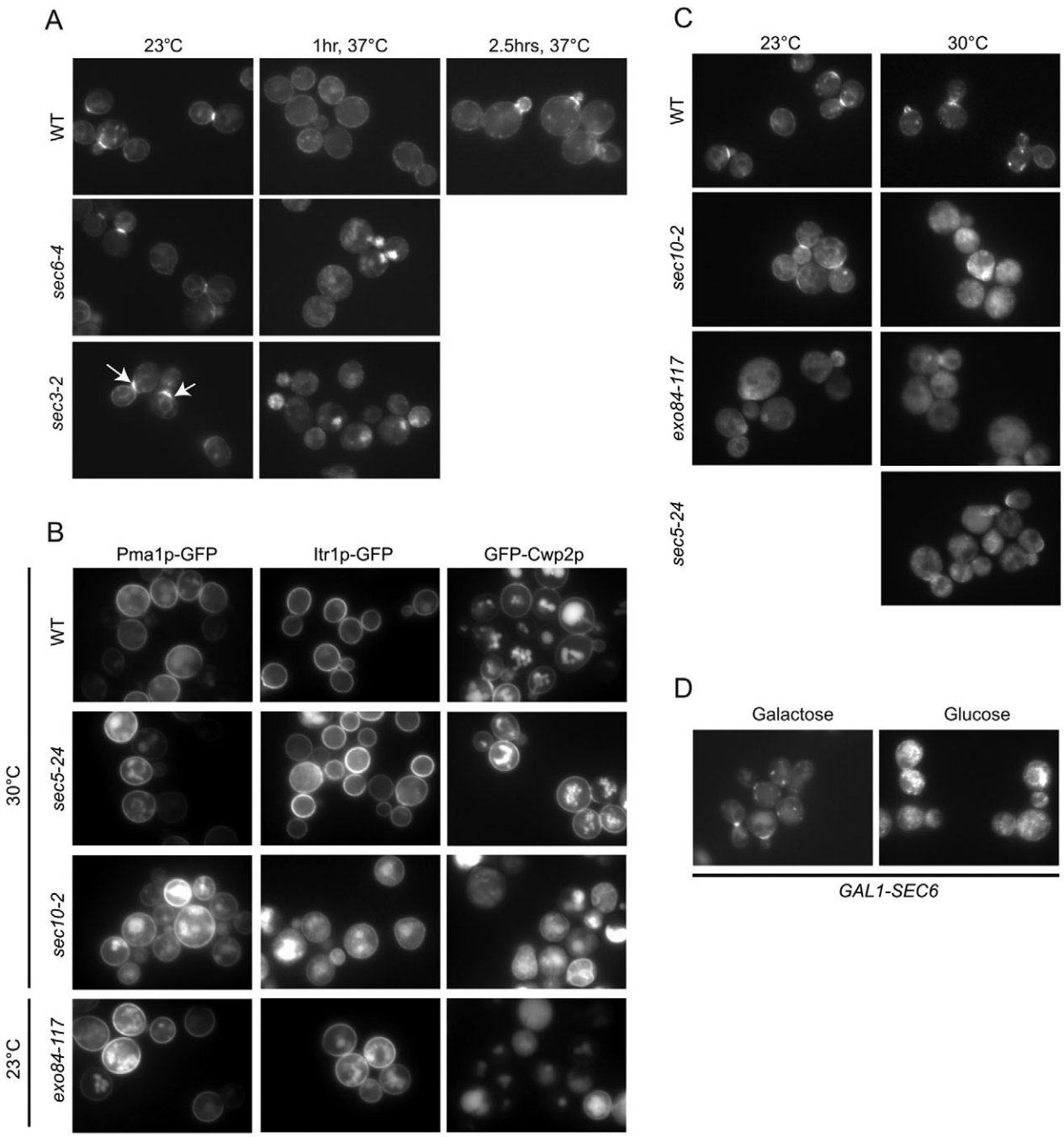

Fig. 3. The exocyst is required for proper plasma membrane localization of Chs3p–GFP and Hxt2p–eqFP611. (**A**) Mutants in the exocyst complex inhibit plasma membrane localization of Chs3p–GFP in response to heat shock. Logarithmically growing cells at 23°C were shifted to 37°C for indicated times and Chs3p–GFP localization was determined by live-cell imaging. The arrows indicate the broader Chs3p–GFP bud-neck localization in *sec3-2* cells at 23°C. (**B**) Plasma membrane localization of Itr1p–GFP and GFP–Cwp2 is impaired at the permissive or semi-permissive temperature in a subset of temperature-sensitive exocyst mutants. Logarithmically growing cells at 23°C were shifted to 30°C for 6 hours, where indicated before analysis. (**C**) Chs3p trafficking is impaired in a subset of exocyst mutants grown at the permissive or semi-permissive temperature. Logarithmically growing cells at 23°C were shifted to 30°C for 6 hours, where indicated before analysis. (**D**) *GAL1* shut-off of *SEC6* leads to intracellular accumulation of Chs3p–GFP. Endogenous *SEC6* was put under the control of the galactose-induced *GAL1* promoter in a strain expressing Chs3p–GFP. Cells grown on galactose were shifted into glucose-containing medium, which causes repression of the *GAL1* promoter. Images were taken 13.5 hours after the shift from galactose into glucose-containing medium.

clustered in the bud neck region early and more pronounced late in the cell cycle. Hence, it is unlikely that both cargoes travel in the same vesicle. Taken together, our data demonstrate that the exocyst is required for the correct localization of Chs3p–GFP at the bud neck. Moreover, they also indicate that similarly to inclusion of Hxt2p and Chs3p in vesicles at the Golgi, fusion at the plasma membrane could also be regulated differently, depending on the cell-cycle stage.

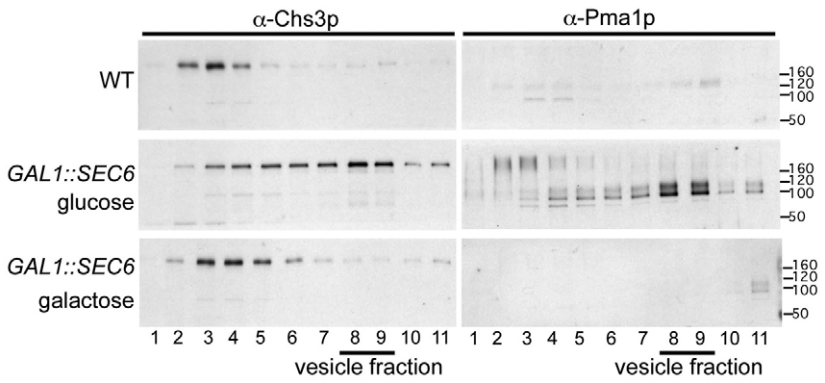

Fig. 4. Chs3p accumulates in the vesicle fraction after *SEC6 GAL1* shut-off. Strains containing *SEC6* under the *GAL1* promoter were incubated for 13 hours in glucose-containing medium, or were cultured in galactose. The supernatant of a 13,000 ***g*** spin was loaded on a sucrose gradient. The gradient fractions were separated by SDS-PAGE, and immunoblots were developed with anti-Chs3p and anti-Pma1p antibodies. The TGN fraction stays close to the top, whereas the vesicle fraction migrates towards the bottom. After *GAL1* shut-off, Chs3p co-migrates with the vesicle fraction containing the plasma membrane ATPase Pma1p, which is not detected without vesicle accumulation.

Sec4p is required for the correct localization of Chs3p

Other key regulators of intracellular traffic are small GTPases of the Rab family, most of which appear to act in post-Golgi traffic in yeast. We wanted to test whether one of the Rab proteins would specifically act on Chs3p–GFP traffic. Only 2 of the 11 Rab proteins in yeast are essential, and conditional mutants are available. Ypt1p is the homologue of Rab1 and is involved in anterograde and retrograde transport in the ER shuttle (Kamena et al., 2008), whereas Sec4p is the Rab required for fusion of transport vesicles with the plasma membrane (Guo et al., 1999). The temperature-sensitive mutant *ypt1-3* did not affect transport of either Chs3p or Hxt2p to the plasma membrane at 23°C (Fig. 6A). By contrast, Chs3p was mislocalized at 37°C, whereas Hxt2p still reached the plasma membrane efficiently. The effect of the *ypt1-3* mutation on Chs3p traffic could be indirect because in this mutant, Golgi morphology and composition is strongly affected (Kamena et al., 2008), to which Chs3p could be more sensitive than Hxt2p.

By contrast, both proteins were affected in *sec4-8* mutant cells at 23°C (Fig. 6) and strong intracellular staining was observed at 37°C. A similar phenotype was observed when we analyzed a mutant in the GEF for Sec4p, Sec2p, indicating that the observed phenotype is specific (Fig. 6B, Table 1). Interestingly, after the shift from high-glucose to low-glucose medium, most Hxt2p was correctly targeted to the plasma membrane at the permissive temperature (Fig. 6C). To corroborate the findings of a role of Sec4p in Chs3p transport, we also analyzed mutants in the non-essential GAPs for Sec4p, Msb3p and Msb4p. Deletion of either *MSB3* or *MSB4* had little to no impact on Hxt2p–eqFP611 and Chs3–pGFP, whereas they were severely mislocalized in *Δmsb3 Δmsb4* (Fig. 6D, Table 1). We conclude that Sec4p and its regulators have a central role in localization of both Chs3p and Hxt2p.

Ypt31p and Ypt32p are required for proper Chs3p–GFP traffic

The function of Ypt1p and Sec4p is central for the transport of all cargo proteins that have to reach the plasma membrane. Therefore, an effect on both cargoes tested here is not unexpected. However, it is conceivable that one of the non-essential Rab proteins could have a more important role in one of the transport pathways than in the others. Therefore, we screened deletion strains of Rab GTPases for localization defects of either Hxt2p or Chs3p. Most of the individual deletions of the Rab GTPases did not impede the localization of Chs3p or Hxt2p (Fig. 7, Table 1). In a *Δypt11* strain, the Chs3p–GFP signal seemed occasionally a bit broader, but Chs3p still reached the bud neck efficiently. Hxt2p transport was affected more than Chs3p plasma membrane localization in a *Δypt7* strain. Ypt7p is the orthologue of Rab7 and is required for all membrane-fusion steps with the yeast lysosome, the vacuole (Fig. 2, Table 1). Although the single deletion of *YPT51* had only mild effects on Chs3p–GFP and Hxt2–eqFP611, loss of all Rab5 activity (*Δypt51 Δypt52 Δypt53*) severely altered the localization of Hxt2p and Chs3p, because neither Chs3p nor Hxt2p could be efficiently endocytosed anymore, and therefore internal structures were almost completely absent (Fig. 7, Table 1). A similar phenotype was observed in a *Δend3* mutant, which is defective in an early phase of endocytosis (supplementary material Fig. S2). As a consequence of failed endocytosis, Chs3p–GFP accumulated at the plasma membrane in medium-sized buds (data not shown). More importantly, when we analyzed *Δypt31* and *Δypt32* mutants, localization of Chs3p–GFP, but not Hxt2p–eqFP611, was impaired (Fig. 7, Table 1). In both mutants, more Chs3p-positive internal structures were visible, which seemed to accumulate sometimes at the bud neck. Moreover, in the temperature-sensitive double mutant, *Δypt31 ypt32A141D*, this phenotype was evident at the permissive temperature (23°C) (Fig. 6, Table 1).

The residence time of Chs3p–GFP is shortened in the small bud neck of *Δypt31* cells

We investigated the phenotype of *Δypt31* and *Δypt32* more closely and determined the level of Chs3p–GFP staining in small-, medium- and large-budded cells. Interestingly, although the levels of Chs3p–GFP in the bud neck of large-budded cells was not altered in *Δypt31* or *Δypt32*, significantly fewer small-budded cells showed correct Chs3p–GFP localization in *Δypt31* cells (Fig. 8A). Because of the large variability of the Chs3p localization in the *Δypt32* strain, we focused our analysis on *Δypt31*. The observed phenotype could be explained by either the lack of transport of Chs3p–GFP to the bud neck in a fraction of cells or a decrease in residence time of Chs3p–GFP in the bud neck of small-budded cells. To distinguish between these possibilities, we performed a time-lapse analysis, for which we took pictures of individual cells every 10 minutes and counted the number of frames in which we could observe a Chs3p–GFP signal in the bud neck of small cells (Fig. 8B,C). These data indicate that the average residence time of Chs3p–GFP is about 1.5 frames (which corresponds to about 15 minutes) shorter in *Δypt31* than in wild-type cells. The initial transport to the bud neck did not seem to be affected in the *Δypt31* mutant, suggesting that either less Chs3p–GFP is transported to the bud neck, or Chs3p–GFP is endocytosed faster from the bud. To distinguish between these possibilities, we measured the intensity of Chs3p–GFP in the bud neck of small-budded wild-type and *Δypt31* cells. However, we did not find any significant differences in the signal intensity in the bud neck (data not shown), favoring the more rapid endocytosis of Chs3p–GFP in the absence

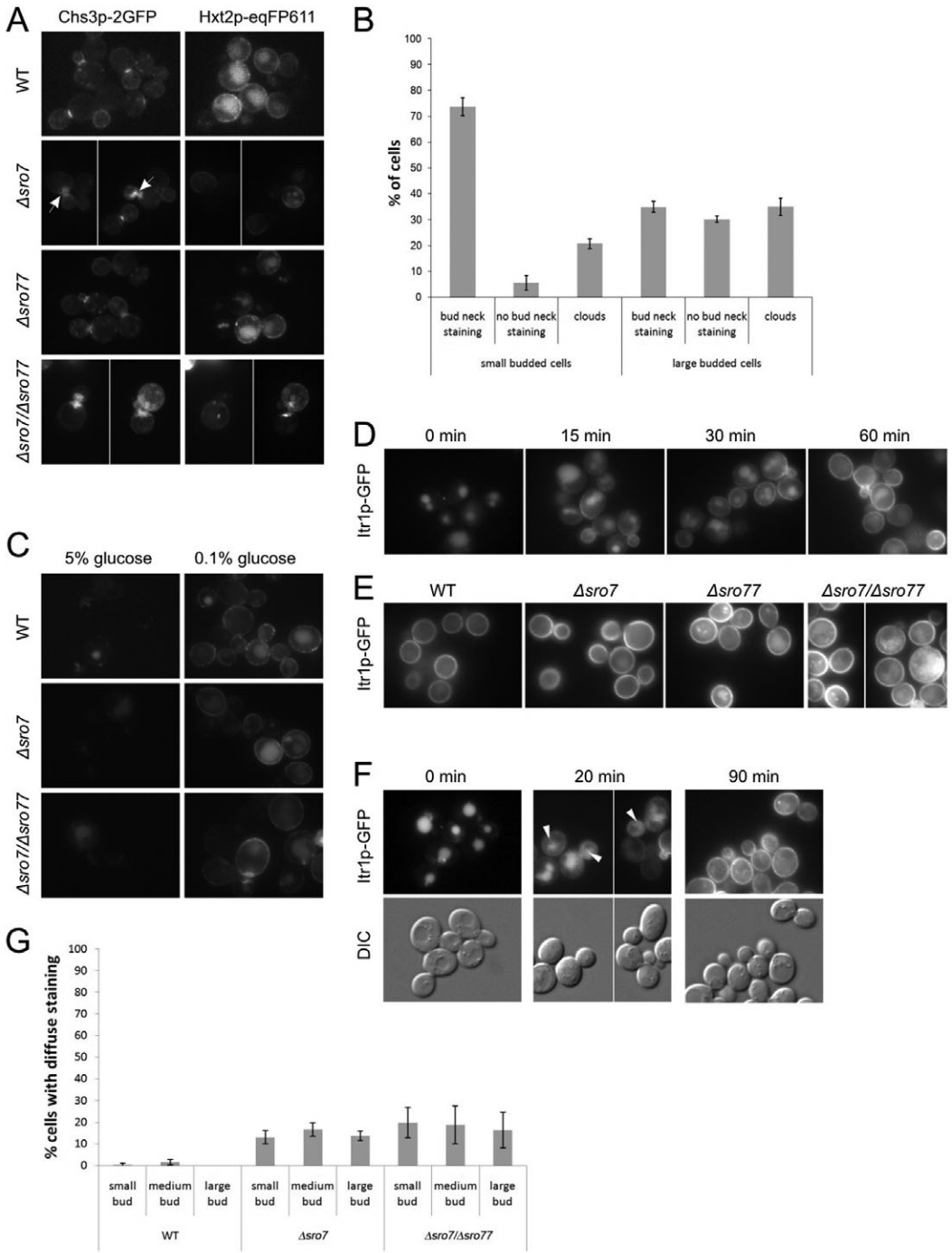

Fig. 5. Sro7p is required for proper bud neck localization of Chs3p especially in large-budded cells. (**A**) *Δsro7* affects trafficking of Chs3p–GFP, but not Hxt2p–eqFP611, to the plasma membrane. Various strains expressing Chs3p–GFP and Hxt2p–eqFP611 were grown to log phase in YPAD at 30°C and subjected to live-cell imaging. The arrows indicate apparent vesicles clouds containing Chs3p–GFP in the bud neck of the *Δsro7* mutant. (**B**) Quantification of the mislocalization of Chs3p–GFP in *Δsro7* cells compared with the wild type. Cells were scored for bud-neck localization of Chs3p–GFP. 'clouds' represents the class of mislocalized Chs3p close to the bud neck. (**C**) Hxt2p–eqFP611 still appears at the plasma membrane in *Δsro7* and in *Δsro7 Δsro77* cells after glucose induction. A high-to-low glucose shift experiment was performed as described in Fig. 2B. (**D**) Itr1p–GFP is transported to the plasma membrane in response to low inositol levels. Cells expressing Itr1p–GFP were grown in YPAD and then shifted into minimal medium, which caused plasma membrane expression of Itr1p–GFP. Pictures were taken 0, 15, 30 and 60 minutes after shift into minimal medium. (**E**) Itr1p–GFP localization at the plasma membrane is only mildly affected in *Δsro7Δsro77* cells under steady state conditions. The localization of Itr1p–GFP was analyzed in WT, *Δsro7*, *Δsro77* and *Δsro7Δsro77* cells grown in minimal medium. (**F**) Itr1p–GFP transport to the plasma membrane is delayed upon induction in *Δsro7* cells. *Δsro7* cells expressing Itr1p–GFP were shifted from rich to minimal medium and the plasma membrane appearance of Itr1p–GFP was followed over time. Initially a haze of Itr1p–GFP signal populated the cytoplasm in some cells. Note that the bright staining represents vacuole-localized Itr1p–GFP. After 90 minutes, Itr1p–GFP was localized at the plasma membrane and was indistinguishable from that in the wild type. The arrowheads point to the haze. (**G**) Quantification of the *Δsro7* and *Δsro7Δsro77* cells that had a delay in Itr1p–GFP transport to the plasma membrane.

of Ypt31p. Because we did not see a difference for the residence time in large-budded cells in the *Δypt31* strain, our data provide evidence that the localization of Chs3p at the bud neck in small-budded cells is regulated in a different manner than in large-budded cells. Furthermore, they suggest that transport to and from a particular location in the cell might require different factors depending on the stage of the cell cycle.

Discussion

We investigated the requirements for plasma membrane localization of Chs3p by conducting a visual screen with mutants of regulators of vesicle fusion at the plasma membrane and Rab GTPases. We found that the requirements for the fusion of transport vesicles containing Chs3p or Hxt2p are mainly the same. However, bud neck localization of Chs3p was specifically affected in *Δsro7*, when compared with Hxt2p, or other exomer-independent cargo such as Itr1p, Pma1p and Cwp2p. Although export of Itr1p to the plasma membrane was delayed in *Δsro7* cells under pulse–chase conditions, no defect was observed under steady-state levels. No role for Sro7p in the formation of transport carriers has been established. It seems to be required rather in later stages of the life cycle of a vesicle, such as the fusion stage. These differences

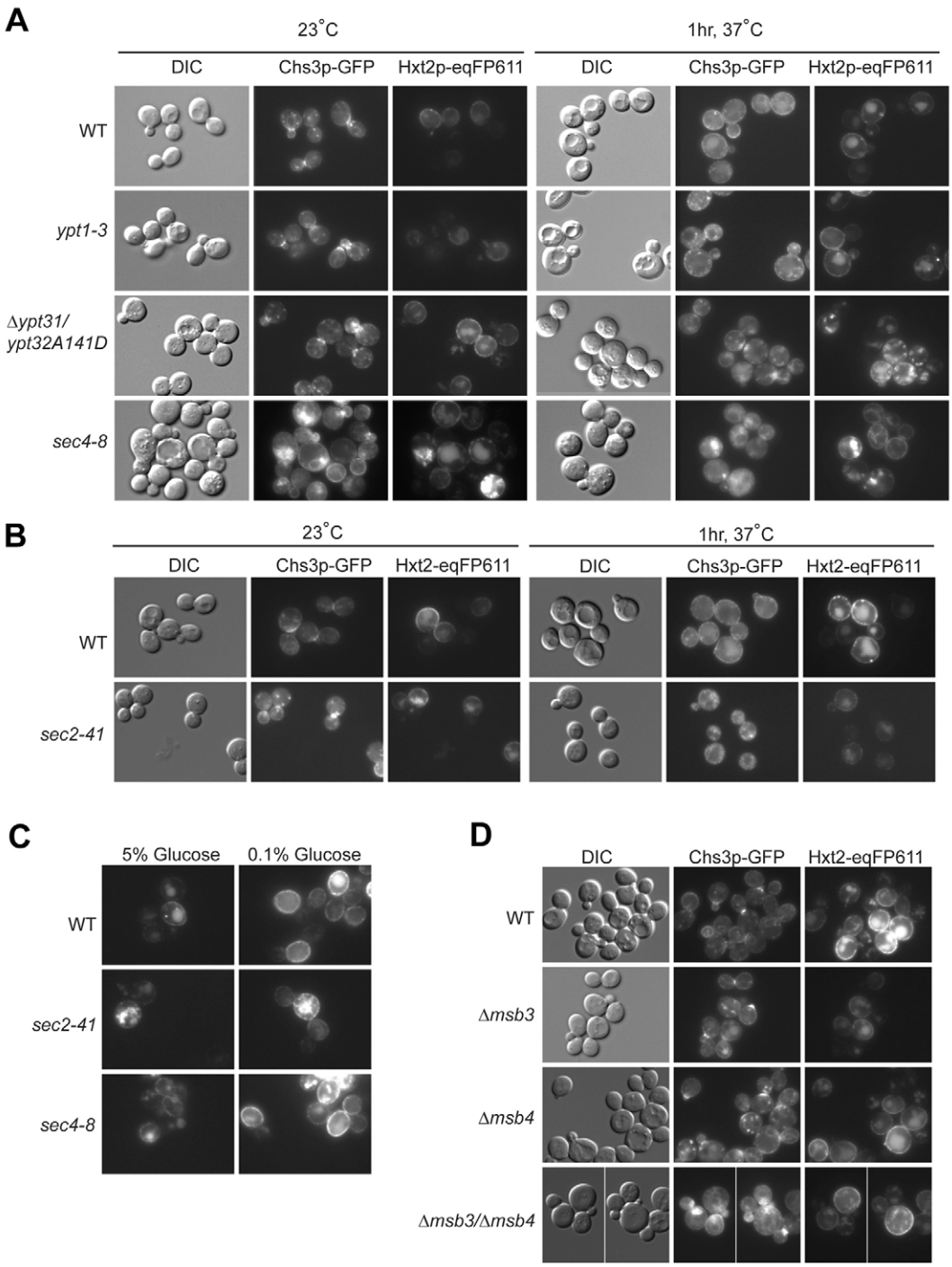

Fig. 6. Several Rab GTPases and the Sec4p GEF influence traffic of cargo to the plasma membrane. (**A**) Strains of the temperature-sensitive mutations of the essential Rab proteins *YPT1* and *SEC4* and the essential pair *YPT31–YPT32* were grown to log phase at 23°C and then shifted to 37°C for 1 hour. Cells were mounted and imaged immediately thereafter. In contrast to *sec4-8*, *ypt1-3* is not required for Chs3p–GFP and Hxt2p–eqFP611 at 23°C. (**B**) *sec2-41* mutant cells are defective in Hxt2p and Chs3p traffic. Wild-type and *sec2-41* strains were grown to log phase at 23°C and then shifted for 1 hour to 37°C. Images were taken immediately after sample preparation. (**C**) *sec4-8* and *sec2-41* are not impaired in Hxt2 transport after glucose shift at 23°C. Cells were grown in 5% glucose, harvested and resuspended in medium containing 0.1% glucose, causing transport of Hxt2p to the plasma membrane. (**D**) The Sec4p-GAPs Msb3p and Msb4p are required for trafficking of Chs3p and Hxt2p–eqFP611 to the bud neck.

suggest either that Chs3p and Hxt2p travel in separate transport containers or that because Chs3p transport is dependent on the cell-cycle state, transport to the plasma membrane is regulated differently according to the cell-cycle phase. These two possibilities are not mutually exclusive and could both operate to control plasma membrane localization of a variety of proteins. Alternatively, a transcytosis type of transport could be envisaged for Chs3p localization. In this scenario, Chs3p would be transported to the bud tip in the same vesicle as Hxt2p and other exomer-independent cargo. Because the bud tip is also the major place for endocytosis, Chs3p could be internalized immediately into special transport containers and routed to the bud neck. There is little evidence for this latter model so far, but it could help explain how the chitin ring can form asymmetrically on the mother-cell side of the neck (DeMarini et al., 1997).

Although we identified mutants that more strongly affected transport to the plasma membrane of Chs3p than of Hxt2p and vice versa, our study does not allow us to definitively conclude the presence of two separate transport containers for Chs3p and Hxt2p. It is likely that the inclusion of Chs3p into nascent vesicles at the TGN is favored at particular times in the cell cycle and that at these times (G1–S phase, cytokinesis) also fusion at the plasma membrane is differently regulated compared with the rest of the cell cycle. Transport of vesicles to the plasma membrane seems to occur by distinct pathways because *cdc42-6* mutants only accumulated vesicles at the restrictive temperature in small-budded but not large-budded cells (Adamo et al., 2001). In contrast to our results, no differential trafficking of cargoes to the plasma membrane was detected. The differential localization patterns for distinct cargoes are probably achieved not only by the fusion of vesicles with the plasma membrane, but also by how quickly the cargo is endocytosed again (Valdez-Taubas and Pelham, 2005).

Interestingly, we found that the residence time of Chs3p at the plasma membrane seems to be regulated differently over the cell cycle, because loss of the Rab11 homologue Ypt31p reduced specifically the time of Chs3p plasma membrane localization in small-budded but not in large-budded cells. We did not detect a reduction in the fluorescence intensity of Chs3p–GFP at the bud neck of *Δypt31* cells, suggesting that the export from the TGN and the arrival at the plasma membrane of Chs3p–GFP are not impaired. Since Sec4p is essential for the fusion of Chs3p-containing transport vesicles, it is unlikely that Ypt31p has a role in the final steps of Chs3p deposition at the plasma membrane. Finally, endocytosis of Chs3p involves the three Rab5 homologues Ypt51p, Ypt52p and Ypt53p, indicating that Ypt31p might not be the determining factor in early steps of Chs3p internalization. However, we cannot definitely exclude a role of Ypt31p in endocytosis, because Singer-Krüger and colleagues (Singer-Krüger et al., 1994) demonstrated no defect in early stages of α-factor receptor endocytosis in *Δypt51Δypt52Δypt53*. Nevertheless, when we tested different cargoes in our triple deletion strain, all cargoes were trapped at the plasma membrane similarly to the phenotype observed in a *Δend3* strain (supplementary material Fig. S2), in which early stages of endocytosis are blocked (Raths et al., 1993). No data are available to our knowledge elucidating the cause of the internalization of Chs3p in G2 phase or after cytokinesis. However, our data suggest that Ypt31p might be a factor contributing to the timely endocytosis of Chs3p, specifically in small-budded cells, for example, early in the cell cycle. Interestingly, Ypt31p is required for the establishment of the bipolar budding pattern in diploid cells (Ni and Snyder, 2001), a function, which is shared by Chs5p and Bud7p. Moreover,

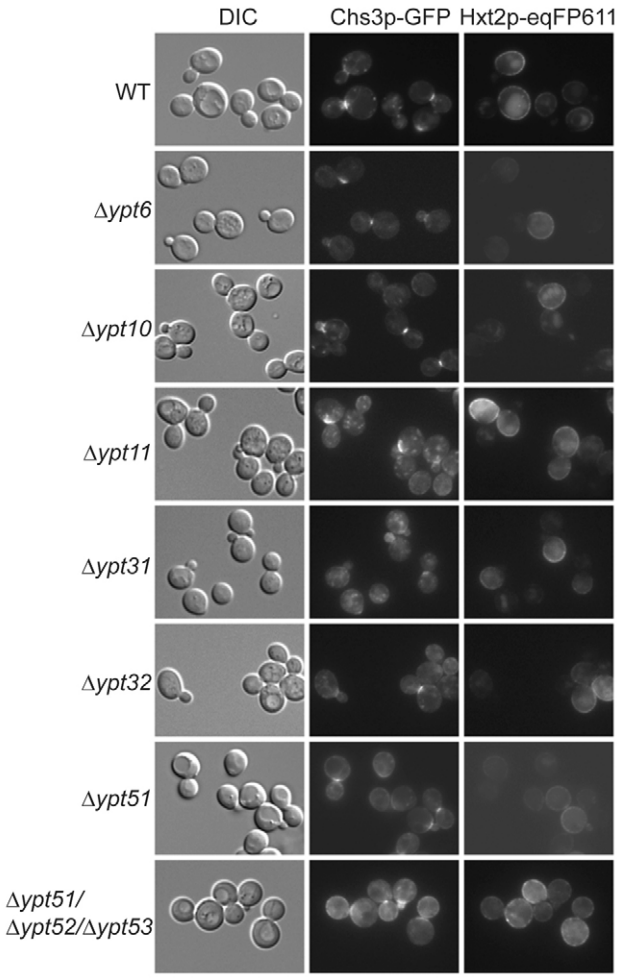

Fig. 7. Analysis of the effect of the deletion of the non-essential Rab proteins on Chs3p and Hxt2p transport. Various Rab genes were deleted in a strain in which Chs3p–GFP and Hxt2p–eqFP611 were expressed. The effect of loss of the Rab proteins on plasma membrane traffic of the markers was assessed after growth of the cells to log phase at 30°C.

Ypt31p localizes to the incipient bud site and to small-budded cells (Jedd et al., 1997), indicating that it might be involved in Chs3p trafficking early in the cell cycle, and that this function could be independent of the function of Ypt31p at the Golgi.

Interestingly, deletion of the lethal giant larva homologue Sro7p specifically interfered with transport of Chs3p to the plasma membrane. Sro77p, which is 54% identical to Sro7p did not have a significant role in transport of either Chs3p or Hxt2p to the plasma membrane. However, simultaneous loss of *SRO7* and *SRO77* resulted in accumulation of both cargoes in internal structures. Although transport to the plasma membrane seems to be heavily impaired, and the double mutant has severe growth defects, *Δsro7 Δsro77* cells still survive. Thus, a Sro7/Sro77p-independent pathway to the plasma membrane must exist. The existence of such a pathway is illustrated by our finding that Hxt2p reaches the plasma membrane efficiently after shift from high to low glucose, which induces Hxt2p expression at the plasma membrane.

The only other implication of Sro7p in the fusion of the specific carriers comes from its initial identification: Sro7p is required for

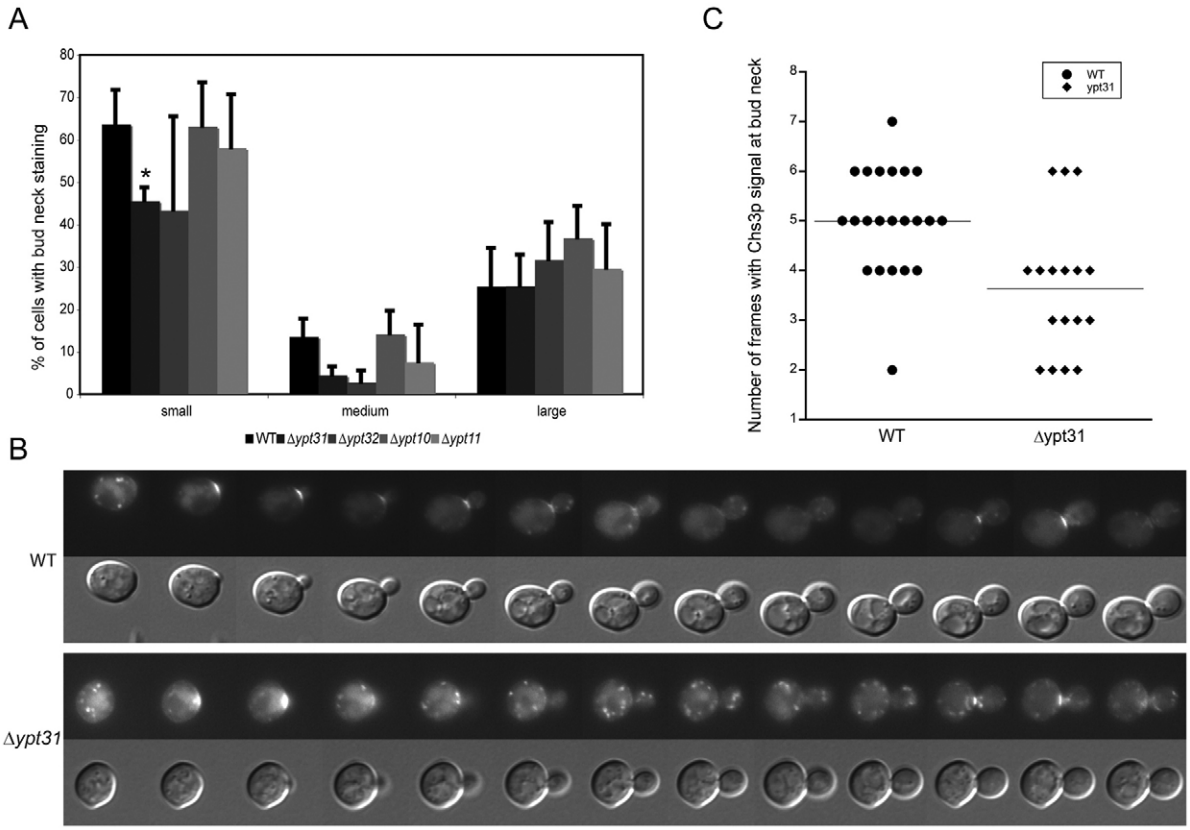

Fig. 8. The residence time of Chs3p–GFP is reduced in the bud neck of small-budded but not large-budded *Δypt31* cells. (**A**) Several *Δrab* strains were grown to log phase and the bud neck localization of Chs3p–GFP was determined in small-, medium- and large-budded cells. Deletion of *YPT31* caused a significant ($P<0.01$; Student's *t*-test) reduction of Chs3p–GFP bud-neck localization specifically in small-budded cells. (**B**) The drop in bud-neck localization in *Δypt31* is due to a shortened residence time of Chs3p at the bud neck. Time-lapse recording of a wild-type cell and a *Δypt31* cell. Although the initial transport of Chs3p–GFP was unaffected, the Chs3p–GFP signal disappears faster from the bud-neck region in *Δypt31* cells. The pictures were taken in 10 minute time intervals. (**C**) Quantification of the effect in B from 22 wild-type and 17 *Δypt31* individual recordings. The difference is statistically significant at $P<0.01$ (Mann-Whitney-U-Test, two-tailed).

the plasma membrane localization of the sodium transporter Ena1p under high-salt stress (Larsson et al., 1998; Wadskog et al., 2006). Our findings, however, show a differential requirement under normal growth conditions. The effect of mislocalization of Chs3p–GFP was more pronounced in large-budded than in small-budded cells. This result reinforces the notion that bud neck localization of Chs3p is governed, at least in part, by different factors during the cell cycle. In addition, it also points to a possible role of exomer-dependent transport in polarity maintenance. The metazoan homologue of Sro7p LGL has been shown to be required for epithelial polarity, and loss of function resulted in epithelial–mesenchymal transition, a key event in metastatic formation of tumors (Reischauer et al., 2009).

Another metazoan homologue, tomosyn, appears to negatively regulate vesicle exocytosis in several systems by regulating the formation of the SNARE complex. By contrast, deletion of *SRO7* led to an accumulation of vesicles containing Chs3p, but not Hxt2p, indicating that formation of SNARE complexes might be impaired in *Δsro7* cells. Our findings are in agreement with a recent report showing that Sro7p promotes SNARE complex assembly (Williams and Novick, 2009). It remains unclear why the vesicle fusion defect in *Δsro7* cells was much more pronounced late in the cell cycle compared with early stages of bud emergence. One possible explanation is that the bud neck is differently organized in small-budded versus large-budded cells (McMurray and Thorner, 2009). During mitosis, the septin collar is split into two rings, one in the mother cell and one in the daughter cell. Chs3p-containing vesicles will have to fuse in between these two rings to synthesize chitin for cytokinesis, whereas most cargo could fuse to either side, and the precise targeting might be not so important. Thus, one of the functions of Sro7p could be to ensure the correct fusion of Chs3p-containing vesicles. This precise targeting might be less important in G1, when the old septin ring from the previous cytokinesis is removed and only one new septin ring is assembled at the emerging bud, which is then transformed in an ordered array, referred to as the septin collar.

Our data suggest that more pathways exist than those previously established for low- and high-density vesicles. The population of low-density vesicles probably consists of several subclasses, one of which is involved in Chs3p transport to the bud neck. A recent report demonstrated the segregation of sphingolipids and sterol during secretory transport vesicle formation (Klemm et al., 2009). However, deletion of two key components in sphingolipid biosynthesis, *ELO3* and *SUR2*, did not differentially affect trafficking of Hxt2p and Chs3p, indicating that sphingolipids would not act as a sorting determinant in our paradigm (Table 1). We cannot exclude the possibility that Hxt2p and Chs3p travel in the same type of vesicles, and sorting at the TGN is the crucial step.

This type of regulation is not unprecedented because different types of COPII vesicles exist, which only can be distinguished by the cargo they transport. For example GPI-anchored proteins are sorted away from other cargo at the ER, but still exit using the COPII machinery (Muniz et al., 2001; Muniz et al., 2000). Moreover, COPI vesicles bud at different levels of the Golgi and hence must also contain different cargo proteins. The finding that only a subset of cargo is misrouted in cells with compromised Golgi function (Kamena et al., 2008) is also consistent with this notion.

Taken together, our results suggest that cargo is sorted in different low-density transport containers at the TGN, and that the fate of a subset of these containers might be regulated differently depending on the cell-cycle state.

Materials and Methods

Yeast methods and antibodies

Standard genetic techniques and media were used throughout (Sherman, 1991). Chromosomal tagging and deletions were performed as described (Gueldener et al., 2002; Janke et al., 2004; Knop et al., 1999). For the chromosomal 3×GFP fusions, we used the template plasmid pYM-3×GFP–TRP1. To construct the template plasmid, 3×GFP along with TRP1 was amplified from plasmid pBS-3×GFP–TRP1 (a gift from John A. Cooper, Washington University, St Louis, MO) and cloned into a pYM7 backbone digested with *Bam*HI–*Sac*I. The Chs3p-2×GFP strain used throughout this study was recovered by a spontaneous loss of one copy of GFP during the homologous recombination. Since we used YPH500/YPH499 as background for all experiments, we introduced mutations either by allelic replacement or through crosses. *sec6-4* and *sec4-8* were cloned into pRS406 (Sikorski and Hieter, 1989) using *Xma*I–*Sac*II. The plasmids were digested with *Bcl*I and transformed into yeast. Positive colonies were subjected to selection on 5-FOA, and temperature-sensitive mutants were used for further analysis. *sec5-24* and *sec10-2* were amplified from strains generously provided by Wei Guo (University of Pennsylvania, PA) and cloned into pRS304 using *Bam*HI and *Not*I. The plasmids were cut with *Nco*I and *Bsr*GI and transformed into yeast. Positive clones were selected on 5-FAA, and temperature-sensitive mutants were used for further analysis. The *exo84-117* mutant strain was constructed by transforming pRS315-*exo84-117* (pGS99; a gift from Wei Guo) into YPH499 and the chromosomal *EXO84* was deleted as described above. The strains used in this study are listed in supplementary material Table S1. The plasmids expressing CPY–GFP, Pma1–GFP and GFP–Cwp2 were generous gifts from Olivier Deloche (University of Geneva, Switzerland), Aaron Neiman (Stony Brook, NY) and Howard Riezman (University of Geneva, Switzerland), respectively. Antibodies against Chs3p and Pma1p have been described earlier (Serrano et al., 1986; Trautwein et al., 2006).

Wide-field microscopy of yeast strains

Strains were grown in YPAD to early to mid-log phase at 23°C or 30°C and shifted to 37°C for various times where indicated. Strains containing a plasmid were grown O/N in HC-URA at 23°C or 30°C, diluted in YPAD and grown for another 4–6 hours at either 23°C or 30°C. Itr1p–GFP strains were grown overnight and diluted in HC complete medium to allow for Itr1p sorting to the plasma membrane. For pulse–chase experiments, strains were grown overnight and diluted in YPAD, grown for 4–6 hours, then harvested and resuspended in HC medium. Cells were harvested by low-speed centrifugation, resuspended in a small volume of HC-complete medium, and an aliquot was spread on a microscope slide. The cells were inspected immediately on an Axioplan 2 microscope equipped with a Axio Cam MRm camera (Carl Zeiss, Aalen Oberkochen, Germany) and a Plan Apochromat 63×/1.40 objective. Axiovision 3.1 software was used to control hardware and to acquire and to process images.

For quantitative analysis, random fields of cells were selected in the DIC channel and pictures were taken in the DIC, GFP and eqFP611 channels. On the DIC image, the cells were classified into small-, medium- and large-budded cells, and then the localization of Chs3p–GFP in the bud neck was scored accordingly using images of the GFP channel.

For time-lapse analysis, cells were mounted onto agarose pads. Images were acquired every 10 minutes at 30°C. Cells were kept in focus by controlling the focal plane either manually or by using the autofocus option in the Axiovision software. The temperature of the slide was controlled using a thermo-controlled stage.

FRAP experiments

Cells were grown on YPD plates, resuspended in liquid non-fluorescent medium and immobilized on non-fluorescent medium (Waddle et al., 1996) containing 1.6% agarose. Imaging was performed on a Zeiss 510 confocal microscope using a Plan-Apochromat 100× objective at room temperature. Fluorescent molecules in the bleaching regions were photobleached. Bleaching regions were irradiated with 250 iterations of 50% laser intensity at 30% output of an argon laser (488 nm) and scans were collected with typically 1% laser intensity under the same condition. Scans were performed before, immediately after and 10 minutes after the bleach.

Gradient separation of secretory vesicles

Strains were precultured in YPD or YP 1% raffinose 1% galactose (YP-GAL). The preculture was then used to inoculate larger cultures in YPD or YP-GAL. For GAL shut-off, strains were grown for 13 hours at 30°C in YPD to reach an OD_{600} of about 0.5. The equivalent of 10 OD_{600} was harvested, resuspended in 200 µl of 10% sucrose (w/w), 20 mM triethanolamine pH 7.2, 1 mM EDTA, 1 mM PMSF, and subjected to glass bead lysis. The lysate was centrifuged at 13,000 ***g*** and 4°C for 6 minutes, and 30 µl of the supernatant was loaded on a 35–60% sucrose step gradient. The gradient was developed by centrifugation for 1 hour at 4°C and 75,000 r.p.m. in a TLA100 rotor (Beckman-Coulter, Krefeld, Germany). Twenty µl fractions were collected from the top and analyzed by immunoblot.

We thank A. Reyes, C. Roncero, J. A. Cooper, O. Deloche, W. Guo, A. Nieman, H. Riezman and R. Schekman for strains and plasmids. Present and past members of the Spang lab are acknowledged for thoughtful discussions and comments. This work was supported by Swiss National Science Foundation, the University of Basel and the ETH Zürich.

Supplementary material available online at
http://jcs.biologists.org/cgi/content/full/124/7/1055/DC1

References

Adamo, J. E., Moskow, J. J., Gladfelter, A. S., Viterbo, D., Lew, D. J. and Brennwald, P. J. (2001). Yeast Cdc42 functions at a late step in exocytosis, specifically during polarized growth of the emerging bud. *J. Cell Biol.* **155**, 581-592.

Bagnat, M. and Simons, K. (2002). Cell surface polarization during yeast mating. *Proc. Natl. Acad. Sci. USA* **99**, 14183-14188.

Barfield, R. M., Fromme, J. C. and Schekman, R. (2009). The exomer coat complex transports Fus1p to the plasma membrane via a novel plasma membrane sorting signal in yeast. *Mol. Biol. Cell* **20**, 4985-4996.

Chuang, J. S. and Schekman, R. W. (1996). Differential trafficking and timed localization of two chitin synthase proteins, Chs2p and Chs3p. *J. Cell Biol.* **135**, 597-610.

DeMarini, D. J., Adams, A. E., Fares, H., De Virgilio, C., Valle, G., Chuang, J. S. and Pringle, J. R. (1997). A septin-based hierarchy of proteins required for localized deposition of chitin in the Saccharomyces cerevisiae cell wall. *J. Cell Biol.* **139**, 75-93.

Gueldener, U., Heinisch, J., Koehler, G. J., Voss, D. and Hegemann, J. H. (2002). A second set of loxP marker cassettes for Cre-mediated multiple gene knockouts in budding yeast. *Nucleic Acids Res.* **30**, e23.

Guo, W., Roth, D., Walch-Solimena, C. and Novick, P. (1999). The exocyst is an effector for Sec4p, targeting secretory vesicles to sites of exocytosis. *EMBO J.* **18**, 1071-1080.

Gurunathan, S., David, D. and Gerst, J. E. (2002). Dynamin and clathrin are required for the biogenesis of a distinct class of secretory vesicles in yeast. *EMBO J.* **21**, 602-614.

Harsay, E. and Bretscher, A. (1995). Parallel secretory pathways to the cell surface in yeast. *J. Cell Biol.* **131**, 297-310.

Harsay, E. and Schekman, R. (2002). A subset of yeast vacuolar protein sorting mutants is blocked in one branch of the exocytic pathway. *J. Cell Biol.* **156**, 271-285.

Janke, C., Magiera, M. M., Rathfelder, N., Taxis, C., Reber, S., Maekawa, H., Moreno-Borchart, A., Doenges, G., Schwob, E., Schiebel, E. et al. (2004). A versatile toolbox for PCR-based tagging of yeast genes: new fluorescent proteins, more markers and promoter substitution cassettes. *Yeast* **21**, 947-962.

Jedd, G., Mulholland, J. and Segev, N. (1997). Two new Ypt GTPases are required for exit from the yeast trans-Golgi compartment. *J. Cell Biol.* **137**, 563-580.

Kamena, F., Diefenbacher, M., Kilchert, C., Schwarz, H. and Spang, A. (2008). Ypt1p is essential for retrograde Golgi-ER transport and for Golgi maintenance in S. cerevisiae. *J. Cell Sci.* **121**, 1293-1302.

Klemm, R. W., Ejsing, C. S., Surma, M. A., Kaiser, H. J., Gerl, M. J., Sampaio, J. L., de Robillard, Q., Ferguson, C., Proszynski, T. J., Shevchenko, A. et al. (2009). Segregation of sphingolipids and sterols during formation of secretory vesicles at the trans-Golgi network. *J. Cell Biol.* **185**, 601-612.

Knop, M., Siegers, K., Pereira, G., Zachariae, W., Winsor, B., Nasmyth, K. and Schiebel, E. (1999). Epitope tagging of yeast genes using a PCR-based strategy: more tags and improved practical routines. *Yeast* **15**, 963-972.

Kruckeberg, A. L., Ye, L., Berden, J. A. and van Dam, K. (1999). Functional expression, quantification and cellular localization of the Hxt2 hexose transporter of Saccharomyces cerevisiae tagged with the green fluorescent protein. *Biochem. J.* **339**, 299-307.

Larsson, K., Bohl, F., Sjostrom, I., Akhtar, N., Strand, D., Mechler, B. M., Grabowski, R. and Adler, L. (1998). The Saccharomyces cerevisiae SOP1 and SOP2 genes, which act in cation homeostasis, can be functionally substituted by the Drosophila lethal(2)giant larvae tumor suppressor gene. *J. Biol. Chem.* **273**, 33610-33618.

Matsuoka, K., Orci, L., Amherdt, M., Bednarek, S. Y., Hamamoto, S., Schekman, R. and Yeung, T. (1998). COPII-coated vesicle formation reconstituted with purified coat proteins and chemically defined liposomes. *Cell* **93**, 263-275.

McMurray, M. A. and Thorner, J. (2009). Septins: molecular partitioning and the generation of cellular asymmetry. *Cell Div.* **4**, 18.

Miyashita, M., Shugyo, M. and Nikawa, J. (2003). Mutational analysis and localization of the inositol transporters of Saccharomyces cerevisiae. *J. Biosci. Bioeng.* **96**, 291-297.

Muniz, M., Nuoffer, C., Hauri, H. P. and Riezman, H. (2000). The Emp24 complex recruits a specific cargo molecule into endoplasmic reticulum-derived vesicles. *J. Cell Biol.* **148**, 925-930.

Muniz, M., Morsomme, P. and Riezman, H. (2001). Protein sorting upon exit from the endoplasmic reticulum. *Cell* **104**, 313-320.

Ni, L. and Snyder, M. (2001). A genomic study of the bipolar bud site selection pattern in Saccharomyces cerevisiae. *Mol. Biol. Cell* **12**, 2147-2170.

Raths, S., Rohrer, J., Crausaz, F. and Riezman, H. (1993). end3 and end4: two mutants defective in receptor-mediated and fluid-phase endocytosis in Saccharomyces cerevisiae. *J. Cell Biol.* **120**, 55-65.

Reischauer, S., Levesque, M. P., Nusslein-Volhard, C. and Sonawane, M. (2009). Lgl2 executes its function as a tumor suppressor by regulating ErbB signaling in the zebrafish epidermis. *PLoS Genet.* **5**, e1000720.

Saksena, S., Wahlman, J., Teis, D., Johnson, A. E. and Emr, S. D. (2009). Functional reconstitution of ESCRT-III assembly and disassembly. *Cell* **136**, 97-109.

Sanchatjate, S. and Schekman, R. (2006). Chs5/6 complex: a multiprotein complex that interacts with and conveys chitin synthase III from the trans-Golgi network to the cell surface. *Mol. Biol. Cell* **17**, 4157-4166.

Serrano, R., Kielland-Brandt, M. C. and Fink, G. R. (1986). Yeast plasma membrane ATPase is essential for growth and has homology with (Na+ + K+), K+- and Ca2+-ATPases. *Nature* **319**, 689-693.

Sherman, F. (1991). Getting started with yeast. *Methods Enzymol.* **194**, 3-21.

Sikorski, R. S. and Hieter, P. (1989). A system of shuttle vectors and yeast host strains designed for efficient manipulation of DNA in Saccharomyces cerevisiae. *Genetics* **122**, 19-27.

Singer-Kruger, B., Stenmark, H., Dusterhoft, A., Philippsen, P., Yoo, J. S., Gallwitz, D. and Zerial, M. (1994). Role of three rab5-like GTPases, Ypt51p, Ypt52p, and Ypt53p, in the endocytic and vacuolar protein sorting pathways of yeast. *J. Cell Biol.* **125**, 283-298.

Spang, A., Matsuoka, K., Hamamoto, S., Schekman, R. and Orci, L. (1998). Coatomer, Arf1p, and nucleotide are required to bud coat protein complex I-coated vesicles from large synthetic liposomes. *Proc. Natl. Acad. Sci. USA* **95**, 11199-11204.

TerBush, D. R. and Novick, P. (1995). Sec6, Sec8, and Sec15 are components of a multisubunit complex which localizes to small bud tips in Saccharomyces cerevisiae. *J. Cell Biol.* **130**, 299-312.

TerBush, D. R., Maurice, T., Roth, D. and Novick, P. (1996). The exocyst is a multiprotein complex required for exocytosis in Saccharomyces cerevisiae. *EMBO J.* **15**, 6483-6494.

Trautwein, M., Schindler, C., Gauss, R., Dengjel, J., Hartmann, E. and Spang, A. (2006). Arf1p, Chs5p and the ChAPs are required for export of specialized cargo from the Golgi. *EMBO J.* **25**, 943-954.

Valdez-Taubas, J. and Pelham, H. (2005). Swf1-dependent palmitoylation of the SNARE Tlg1 prevents its ubiquitination and degradation. *EMBO J.* **24**, 2524-2532.

Valdivia, R. H. and Schekman, R. (2003). The yeasts Rho1p and Pkc1p regulate the transport of chitin synthase III (Chs3p) from internal stores to the plasma membrane. *Proc. Natl. Acad. Sci. USA* **100**, 10287-10292.

Valdivia, R. H., Baggott, D., Chuang, J. S. and Schekman, R. W. (2002). The yeast clathrin adaptor protein complex 1 is required for the efficient retention of a subset of late Golgi membrane proteins. *Dev. Cell* **2**, 283-294.

Waddle, J. A., Karpova, T. S., Waterston, R. H. and Cooper, J. A. (1996). Movement of cortical actin patches in yeast. *J. Cell Biol.* **132**, 861-870.

Wadskog, I., Forsmark, A., Rossi, G., Konopka, C., Oyen, M., Goksor, M., Ronne, H., Brennwald, P. and Adler, L. (2006). The yeast tumor suppressor homologue Sro7p is required for targeting of the sodium pumping ATPase to the cell surface. *Mol. Biol. Cell* **17**, 4988-5003.

Wang, C. W., Hamamoto, S., Orci, L. and Schekman, R. (2006). Exomer: a coat complex for transport of select membrane proteins from the trans-Golgi network to the plasma membrane in yeast. *J. Cell Biol.* **174**, 973-983.

Wiedenmann, J., Schenk, A., Rocker, C., Girod, A., Spindler, K. D. and Nienhaus, G. U. (2002). A far-red fluorescent protein with fast maturation and reduced oligomerization tendency from *Entacmaea quadricolor* (Anthozoa, Actinaria). *Proc. Natl. Acad. Sci. USA* **99**, 11646-11651.

Williams, D. C. and Novick, P. J. (2009). Analysis of SEC9 suppression reveals a relationship of SNARE function to cell physiology. *PLoS One* **4**, e5449.

Ziman, M., Chuang, J. S. and Schekman, R. W. (1996). Chs1p and Chs3p, two proteins involved in chitin synthesis, populate a compartment of the Saccharomyces cerevisiae endocytic pathway. *Mol. Biol. Cell* **7**, 1909-1919.